

MHD SIMULATIONS OF A MOVING SUBCLUMP WITH HEAT CONDUCTION

NAOKI ASAI¹, NAOYA FUKUDA², AND RYOJI MATSUMOTO³

¹ Graduate School of Science and Technology, Chiba University, 1-33 Yayoi-cho, Inage-ku, Chiba 263-8522, Japan

² Dept. of Computer Simulation, Faculty of Informatics, Okayama University of Science, 1-1 Ridai-cho, Okayama 700-0005, Japan

³ Department of Physics, Faculty of Science, Chiba University, 1-33 Yayoi-cho, Inage-ku, Chiba 263-8522, Japan
E-mail: asai@astro.s.chiba-u.ac.jp, fukudany@sp.ous.ac.jp, matumoto@astro.s.chiba-u.ac.jp

ABSTRACT

High resolution observations of cluster of galaxies by *Chandra* have revealed the existence of an X-ray emitting *comet-like* galaxy C153 in the core of cluster of galaxies A2125. The galaxy C153 moving fast in the cluster core has a distinct X-ray tail on one side, obviously due to ram pressure stripping, since the galaxy C153 crossed the central region of A2125. The X-ray emitting plasma in the tail is substantially cooler than the ambient plasma. We present results of two-dimensional magnetohydrodynamic simulations of the time evolution of a subclump like C153 moving in magnetized intergalactic matter. Anisotropic heat conduction is included. We found that the magnetic fields are essential for the existence of the cool X-ray tail, because in non-magnetized plasma the cooler subclump tail is heated up by isotropic heat conduction from the hot ambient plasma and does not form such a *comet-like* tail.

Key words : clusters of galaxies – conduction – magnetic fields – MHD – X-ray

I. INTRODUCTION

High spatial resolution observations of central region of cluster of galaxies by *Chandra* have revealed the existence of a peculiar X-ray emitting *comet-like* structure.

Wang *et al.* (2004) presented results of a deep *Chandra* observation together with extensive multi-wavelength data of large-scale hierarchical structure related with A2125. An interesting feature is a distinct X-ray tail on one side of the fast moving ($v \sim 1500 \text{ km s}^{-1}$) galaxy C153, probably created by ram pressure stripping. They suggested that C153 crossed the central region of A2125 containing cD-like elliptical galaxies quite recently. Since X-ray emission above 1.5 keV is absent in this tail, this tail is substantially cooler ($kT \leq 1.5 \text{ keV}$) than ambient intergalactic plasmas ($kT \sim 3.2 \text{ keV}$). They estimated that the length of this trail is $\sim 22''$ ($\sim 88 \text{ kpc}$) and its average width is $\sim 4''$ ($\sim 16 \text{ kpc}$). Additionally, an extended [O II] line emission toward the same direction has been detected.

Since heat conduction in cluster of galaxies can be very efficient (e.g., Takahara & Ikeuchi 1977), heat conduction plays a key role in the formation of cold fronts (e.g., Etori & Fabian 2000; Vikhlinin *et al.* 2001) and thermal balance in the cluster core (cooling flow problem). Asai *et al.* (2004) showed the dramatic effect of magnetic fields on heat conduction in cluster of galaxies. They carried out magnetohydrodynamic (MHD) simulations of a subcluster moving in a magnetized intercluster plasma. They showed that the contact sur-

face (a cold front) between the cool subcluster plasma and hot intercluster plasma is maintained because the heat conduction across the cold front is suppressed by magnetic fields wrapping the forehead of the moving subcluster. In non-magnetized plasma, however, the cold front disappears by heat conduction. Similarly, the cool X-ray tail embedded in hotter ambient plasma should subject to heating by thermal conduction.

In this paper, we investigate the interaction between a moving subclump and magnetized intergalactic plasma and explore necessary conditions for the existence of the cool X-ray trail.

II. SIMULATION MODEL

We simulated the time evolution of a subclump in a frame comoving with the subclump. We solve the two-dimensional (2D) resistive MHD equations in a Cartesian coordinate system (x, y). We use the specific heat ratio $\gamma = 5/3$. We assume an anomalous resistivity. The resistivity sets in locally only when the drift velocity ($v_d \equiv |j|/\rho$) exceeds the critical velocity (v_c), where j is current density. When $v_d \geq v_c$, the resistivity is $\eta = \eta_0(v_d/v_c - 1)^2$, otherwise $\eta = 0$. We adopt $\eta_0 = 0.01$ and $v_c = 3.0$. We set an upper limit of the resistivity, $\eta_{\text{max}} = 1.0$. We assume heat conduction along the magnetic field line. The classical Spitzer conductivity (Spitzer 1962) is assumed. When magnetic fields exist, the conductivity along the field line is $\kappa \approx \kappa_{\parallel} = \kappa_0 T^{5/2}$ ($\kappa_0 = 5 \times 10^{-7} \text{ ergs s}^{-1} \text{ cm}^{-1} \text{ K}^{-1}$) and the conductivity across the field line is $\kappa_{\perp} = 0$, where T is temperature.

The size of the computational box is $600 \text{ kpc} \times 400 \text{ kpc}$ and the number of grid points is $(N_x, N_y) = (1200, 800)$.

The units of length, velocity, density, pressure, temperature, and time in our simulations are $r_0 = 25 \text{ kpc}$, $v_0 = 500 \text{ km s}^{-1}$, $\rho_0 = 6.5 \times 10^{-27} \text{ g cm}^{-3}$, $p_0 = 4 \times 10^{-11} \text{ erg cm}^{-3}$, $T_0 = 1.5 \text{ keV}$, and $t_0 = r_0/v_0 = 5 \times 10^7 \text{ yr}$, respectively.

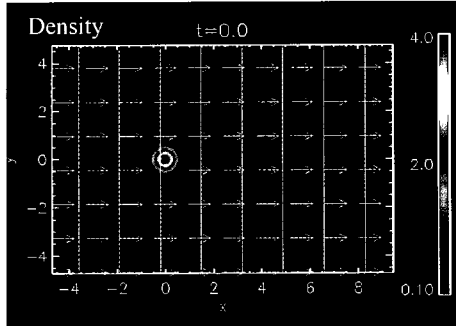


Fig. 1.— Initial density distribution (color scale) in the central region ($375 \text{ kpc} \times 250 \text{ kpc}$) of simulation box. Solid lines show magnetic field lines and arrows show velocity vectors.

Figure 1 shows the initial density distribution in the central region ($375 \text{ kpc} \times 250 \text{ kpc}$). Solid lines and arrows show magnetic field lines and velocity vectors. The subclump is assumed to be a spherical isothermal low-temperature ($kT_{\text{in}} = 1.5 \text{ keV}$) plasma confined by the gravitational potential of the subclump. It is embedded in the less-dense ($\rho_{\text{out}} = 0.25 \rho_0$), uniform hot ($kT_{\text{out}} = 3.0 \text{ keV}$) plasma. Here the subscripts “in” and “out” denote the values inside and outside the subclump, respectively. We assume that the density distribution of the subclump is given by the β -model profile, $\rho_{\text{in}} = \rho_c [1 + (r/r_c)^2]^{-3\beta/2}$, where $r = (x^2 + y^2)^{1/2}$ and $\beta = 2/3$. The maximum density is $\rho_c = 5\rho_0 = 3.2 \times 10^{-26} \text{ g cm}^{-3}$, and the core radius is $r_c = 8.3 \text{ kpc}$. The subclump is initially in hydrostatic equilibrium under the gravitational potential fixed throughout the simulation.

Table 1 shows model parameters. Important parameter is the plasma beta (β_0) defined as the ratio of the ambient gas pressure to the magnetic pressure. When $\beta_0 = p_{\text{gas}}/p_{\text{mag}} = 100$, the magnetic field strength is $B \sim 3 \mu\text{G}$.

We assume that the ambient plasma initially has a uniform speed with Mach number $M = v_x/c_{s,\text{out}} = 1$, where $c_{s,\text{out}}$ is the ambient sound speed. The Mach number with respect to the sound velocity inside the subcluster is $M' = v_x/c_{s,\text{in}} = \sqrt{2}$.

Model HC is a non-magnetic model with isotropic heat conduction. Models MCA, MCB, and MCC are models with moderate magnetic fields ($\beta_0 = 100$) and anisotropic heat conduction. In models HC, MCB, and MCC, the Mach number is taken to be $M = 2$, and in model MCA, it is taken to be $M = 1$. The inclina-

tion of magnetic fields from motion of the subclump is parameterized by $\theta = \arccos[\mathbf{v} \cdot \mathbf{B}/(vB)]$.

We use a modified Lax-Wendroff method with artificial viscosity for MHD part, and the heat conduction term in energy equation is solved by the implicit red and black successive overrelaxation method (see Yokoyama & Shibata 2001 for details).

For boundary conditions, the left boundary at $x = -5$ is taken to be a fixed boundary, and other boundaries are taken to be free boundaries where waves can be transmitted.

III. NUMERICAL RESULTS

(a) Effects of Magnetic Fields on Cold X-Ray Tail

Let us investigate effects of magnetic fields on the existence of the cold X-ray tail. Figure 2 shows the results for models MCA, MCB, MCC, and HC from left to right, respectively. The top and bottom panels in Figure 2 show the distributions of temperature and X-ray intensity at the central region ($375 \text{ kpc} \times 250 \text{ kpc}$) after $t = 2 \times 10^8 \text{ yr}$. X-ray intensity is visualized from simulation results as logarithm of $\sim \rho^2$.

In models with magnetic fields (MCA, MCB, and MCC), the cold plasma inside the subclump is expelled backward due to ram pressure and forms a cool tail dividing into two branches. The cool tail survives the heat conduction from hotter ambient plasmas, because magnetic fields wrapping the subclump suppress the heat conduction across them. On the other hand, in a model without magnetic fields (model HC), cool plasmas inside the subclump is heated by thermal conduction and evaporates quickly. Thus cool tail is not formed in this model.

In all models with magnetic fields, magnetic fields accumulating ahead of the subclump form a magnetic shield (e.g., Miniati *et al.* 1999) and their strength is enhanced several times that of the initial state. In addition to the suppression of heat conduction, magnetic fields also prevent the Kelvin-Helmholtz instability in this region.

A typical length of the X-ray tail formed in our sim-

Table 1. Models and parameters. Heat conduction is isotropic in model HC. In other models, heat conducts only along magnetic fields. θ is an angle between the motion of the subclump and the magnetic field.

Model	$\theta [^\circ]$	β_0	κ	Mach number
MCA	90	100	κ_{\parallel}	1
MCB	90	100	κ_{\parallel}	2
MCC	45	100	κ_{\parallel}	2
HC	—	∞	κ	2

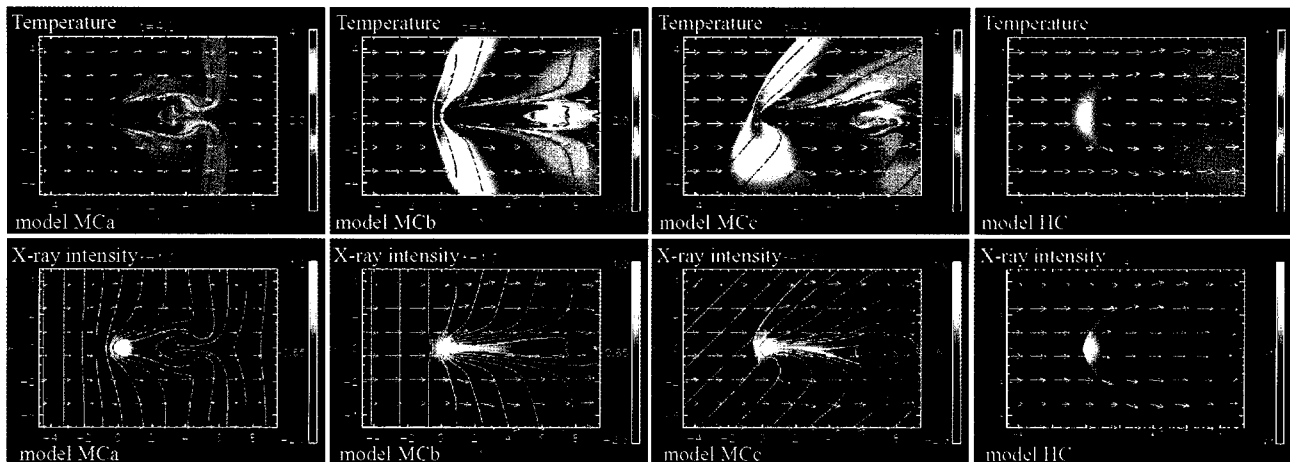


Fig. 2.— Results for models MCa, MCb, MCc, and HC from left to right, respectively. The top and bottom panels show distribution of temperature (*top*) and X-ray intensity (*bottom*) at the central region ($375 \text{ kpc} \times 250 \text{ kpc}$) after $t = 2 \times 10^8 \text{ yr}$, respectively. Solid curves show the magnetic field lines and arrows show the velocity vectors.

ulation is $100 - 200 \text{ kpc}$, and its width is $25 - 50 \text{ kpc}$ at $t = 2 \times 10^8 \text{ yr}$. The tails are longer in models MCb and MCc (Mach number $M = 2$), than model MCa (Mach number $M = 1$), because the subclump subjects to the stronger ram pressure.

(b) Effects of Magnetic Fields on Energy Conversion

When a subclump moves in magnetized plasmas, magnetic fields can extract the kinetic energy of the plasma moving with the subclump because magnetic field lines are stretched by the plasma moving with the subclump. The kinetic energy is converted to magnetic energy and thermal energy. We computed the energy conversion rates in order to study whether a motion of a subclump heats the ambient plasma. Figure 3 shows the time evolution of magnetic (*solid line*), kinetic (*dotted line*), and thermal (*dot-dashed line*) energies with respect to the initial kinetic energy, respectively. The left and right panels show results for model MCb (with magnetic fields) and HC (without magnetic fields).

The left panel shows that magnetic energy increases only slightly, because magnetic fields are deformed in small area close to the subclump. On the other hand, thermal energy increases while kinetic energy decreases. That is, the kinetic energy of the subclump is converted into thermal energy through a shock heating. The right panel shows the similar behavior in model HC.

The inefficiency of the energy conversion from kinetic energy to magnetic energy is partly due to the free boundary condition. When the magnetic fields are fixed at the boundaries, magnetic fields will be deformed until magnetic energy is comparable to the gravitational energy.

IV. DISCUSSION & SUMMARY

We carried out 2D MHD simulations of a subclump moving through a magnetized ambient plasma. In

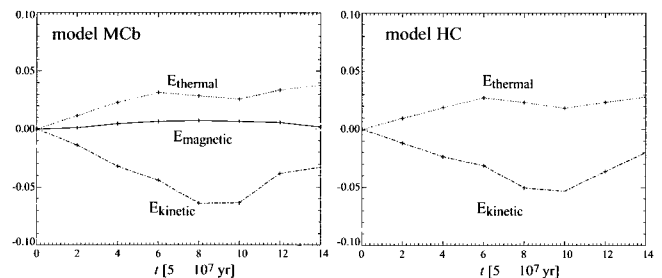


Fig. 3.— Time evolutions of magnetic (*solid line*), kinetic (*dot-dashed line*), and thermal (*dotted line*) energies integrated for the whole simulation region, respectively. Left: Results for model MCb (with magnetic fields). Right: Results for model HC (without magnetic fields).

§III(a), we showed that the magnetic field is essential for the existence of a cold X-ray tail of a subclump like the galaxy C153 observed in A2125. Heat conduction across the magnetic fields is suppressed by the magnetic field wrapping the subclump. This mechanism is the same as that which enables the maintenance of cold fronts in cluster of galaxies (Asai *et al.* 2004).

In the context of interstellar matter, similar works have been done (e.g., Jones *et al.* 1996; Miniati *et al.* 1999), although heat conduction and gravity are not included in their simulations.

They investigated, through 2D MHD simulations, the interaction of a uniform magnetic field oblique to a moving interstellar cloud. Miniati *et al.* (1999) discussed the conversion rate of kinetic energy to magnetic energy for several models. In contrast to their results, only a small fraction of the kinetic energy is converted to the magnetic energy in our models (see §III(b)). The difference comes mainly from the fact that a subclump in our model has lower density and moves faster than that in their model.

Makishima *et al.* (2001) proposed a model of heating of cluster plasma through the motion of member galaxies in magnetic fields. In local simulations we pre-

sented in this paper, the energy conversion rate of kinetic energy of the moving subclump to the magnetic energy is small because magnetic fields can freely move at boundaries. In cluster of galaxies, magnetic fields may be anchored to the cD galaxies. When subclumps move in such magnetosphere of the cD galaxy, magnetic fields will be stretched and twisted. Under such situation, the kinetic energy of the dark matter clump will be extracted through the magnetic interaction. The deformed magnetic field lines may form current sheets, in which magnetic reconnection converts magnetic energy into thermal energy and kinetic energy. We expect efficient heating through this process. This mechanism can be the heat source which compensates for the radiative cooling in cluster plasmas. Obviously, we have to carry out global MHD simulations to study this process. We would like to report the results of such simulations in subsequent papers (Asai *et al.* 2005 in preparation).

ACKNOWLEDGEMENTS

We thank T. Yokoyama for developments of the coordinated astronomical numerical software (CANS) which include 2D MHD codes including heat conduction. The development of CANS was supported by ACT-JST of Japan Science and Technology Corporation. This work is supported by the priority research project in graduate school of Science and Technology, Chiba University (P.I., R. Matsumoto). Numerical computations are carried out by VPP5000 at NAOJ.

REFERENCES

- Asai, N., Fukuda, N., & Matsumoto, R. 2004, *ApJ*, 606, L105
Asai et al. 2005, in preparation.
Ettori, S., & Fabian, A. C. 2000, *MNRAS*, 317, L57
Fabian, A. C. 1994, *ARA&A*, 32, 277
Ikebe, Y., et al. 1997, *ApJ*, 481, 660
Jones, T. W., Ryu, D., & Tregillis, I. L. 1996, *ApJ*, 473, 365
Makishima, K., et al. 2001, *PASJ*, 53, 401
Miniati, F., Jones, T. W., & Ryu, D. 1999, *ApJ*, 517, 242
Peterson, J. R., et al. 2001, *A&A*, 365, L104
Spitzer, L. 1962, *Physics of Fully Ionized Gases* (2d ed.; New York: Interscience)
Takahara, F., & Ikeuchi, S. 1977, *Prog. Theor. Phys.*, 58, 1728
Vikhlinin, A., Markevitch, M., & Murray, S. S. 2001, *ApJ*, 551, 160
Wang, Q. D., Owen, F., & Ledlow, M. 2004, *ApJ*, 611, 821
Yokoyama, T., & Shibata, K. 2001, *ApJ*, 549, 1160